

MICROSTRUCTURE AND THERMOPROPERTIES OF N-OCTADECANE DURING PHASE TRANSITION: A MOLECULAR DYNAMICS SIMULATION

S. K. ZHANG, H. F. LI, Y. HE, Y. HE, Y. ZHOU*

College of Mechanical and Electrical Engineering, Qingdao University of Science and Technology

The thermophysical properties and microstructure of n-octadecane with crystalline and amorphous were investigated by employing the molecular dynamics (MD) simulation. The distribution of the end to end distance and bond torsion angle of the n-octadecane molecular chain and the mean square displacement and thermal conductivity before and after phase transition were also examined. MD simulation results indicates that the molecular chain conformation of amorphous n-octadecane in solid state is gradually changed from stretching to torsion by increasing temperature, and the chains will stretch out as the temperature rises in the liquid state. Compared with amorphous paraffin, the diffusion coefficient and the phase transition temperature of crystalline paraffin is lower than that of amorphous paraffin. The thermal conductivity of crystalline paraffin is much higher than that of amorphous paraffin. It is shown that improving the order degree of PCMs is an effective method to enhance their thermophysical properties.

(Received August 30, 2020; Accepted January 5, 2021)

Keywords: MD simulation, Phase change materials, Thermal physical properties, Microstructure

1. Introduction

Studies for the phase change materials (PCM) is an important part of the development of energy storage technology which is an effective way to deal with environmental pollution and energy crisis.[1-3] Paraffin-based PCM, mainly composed of straight chain alkanes, have been applied to thermal management for their strong heat storage and release properties.[4] However, the application of paraffin-based PCM in the industry field is limited by their the low thermal conductivity.⁵ For the aim to improve the thermophysical properties, high thermal conductivity materials, including carbon nanomaterials, metal nanoparticles, metal foams and other additives, were used to prepare composite phase change materials (CPCM) with various experimental methods in previous studies.[6-12]

In recent decades, a large number of review articles on the preparation, characterization and application of PCM have been published. The main research methods in the past are experiment and numerical calculation or simulation (mostly in macro perspective). Karaipekli et al. [13] tried to improve the thermal conductivity of expanded perlite/paraffin (EXP/C20) CPCM by adding CNT. They also found that the thermal conductivity increases to 0.19, 0.24 and 0.28 W/(m K) when the CNT mass fraction is 0.3%, 0.5% and 1% respectively. Yu et al. [14] prepared a sort of novel PCM microcapsules based on n-octadecane core and calcium carbonate (CaCO₃) shell which present a well-defined core-shell structure. The result shows that the microencapsulated n-octadecane also exhibited excellent phase-change performance and achieved a high thermal storage capability, and however, their encapsulation ratio and encapsulation efficiency were determined by the core/shell mass ratio. Huang et al. [15] compared the effects of graphene and graphene oxide additives on the thermophysical properties of paraffin by MD simulation. From the vibration power spectrum of paraffin, graphene and graphene oxide, it was found that there was vibration coupling between paraffin, graphene and graphene oxide in the middle and low frequency region. The molecular vibration coupling forms the heat transfer channel for the graphene/paraffin and graphene oxide/paraffin interface. In addition, compared

* Corresponding author: zhouyanqd@163.com

with paraffin/graphene, the thermal conductivity of paraffin/graphene oxide is higher than that of paraffin/graphene due to their larger molecular vibration coupling.

The above research focuses on the thermophysical properties and phase transition characteristics of CPCM, but little on the change of microstructure during phase transition. And MD simulation is good at studying microstructure characteristics. Hasan babaei et al. [16] investigated the relationship between the microstructure and thermophysical properties of solid and liquid paraffin by MD simulation. The results show that the structural order degree and thermal conductivity will be improved by CNT and GNP. It is not only due to the existence of high thermal conductivity additives, but also to the addition of carbon nano-fillers will provide a platform for paraffin molecular directional crystallization. Liu et al. [17] carried out MD simulation study on the paraffin/copper nanosheets and paraffin/carbon nanotubes/copper nanosheets, and they observed the structural changes and thermal properties during the simulation process. The results show that the copper nanosheets addition to paraffin crystallization is favorable by improving the thermal conductivity of the system. The addition of CNT makes the alkane molecules in the vicinity more orderly.

In this work, the thermophysical properties and microstructure of crystalline paraffin and amorphous paraffin in the process of phase transition will be studied by MD simulations. The end to end distance and bond torsion angle distribution, self-diffusion coefficient and thermal conductivity will be examined. It is hoped that these result can provide a reference for the microstructure and performance for paraffin in the heat storage system.

2. Model and method

In this paper, the MD method which accords with the classical Newton's law of motion is used to study the microstructure and thermophysical properties of n-octadecane. According to the published literature [15-17], COMPASS (condensed phase optimized molecular potentials for atomic simulation study) can be successfully used to study organic and inorganic materials. As an ab initio force field [18], COMPASS force field can be successfully used to calculate the properties of alkane systems, [19] it can be described by the following formula:

$$E_{\text{total}} = E_{\text{bond}} + E_{\text{angle}} + E_{\text{oop}} + E_{\text{torsion}} + E_{\text{cross}} + E_{\text{elec}} + E_{\text{lj}} \quad (1)$$

E_{total} can be divided into bond interaction term and non-bond interaction term. E_{bond} represents the bond stretching energy, E_{angle} represents the bond angle bending energy, E_{oop} , E_{torsion} and E_{cross} represent the out-off-plane, bond torsion energy and cross term interaction energy respectively, which constitute the bond interaction term. E_{elec} and E_{lj} constitute non-bond interaction term, which represents electrostatic interaction and van der Waals interaction respectively.

In the research, straight chain alkane n-octadecane ($C_{18}H_{38}$) was used to represent paraffin molecule, and two different initial structures have been constructed through Amorphous Cell module based on the COMPASS force field, as shown in Figure1. The two system contains 36 n-octadecane molecules, of which the system "Amorphous" is amorphous structure and the system "Crystal" is a crystalline structure aligned along the Z axis. Periodic boundary conditions are adopted for each system, and the initial temperature is set at 280 K.

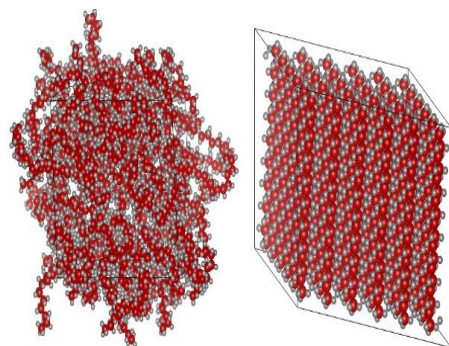


Fig. 1. Amorphous structure and crystalline structure of *n*-octadecane molecules (red balls are carbon atoms; gray balls are hydrogen atoms).

After the initial configuration of each system is established, it is necessary to conduct pretreatment for the system in order to obtain a more reasonable structure. The smart minimization method is used to optimize the structure of the system. Then the anneal dynamics simulations were performed from 280 K to 330 K under the NPT ensemble. The 10 ps dynamics of every 10 K was calculated, and the total simulation time of the five cycle was 500 ps. The kinetic energy, potential energy, non-bond energy, and total energy fluctuation curves of each system during anneal cycles is shown in Figure 2. After annealing, the optimal model of each system is selected as the initial configuration of the dynamic heating process. A dynamic simulation is carried out for each system under the NPT ensemble every 10 K from the 280 K-330 K temperature range. The simulated time at each temperature is 1000 ps. The pressure was set at 0.0001 GPa and the time step was 1 fs. Andersen and Berendsen were used to control temperature and pressure, Atom based and Ewald methods were used to calculate van der Waals interaction and electrostatic interaction respectively. All the data were collected every 0.1 ps, the initial velocity of each particle is sampled according to Maxwell distribution.

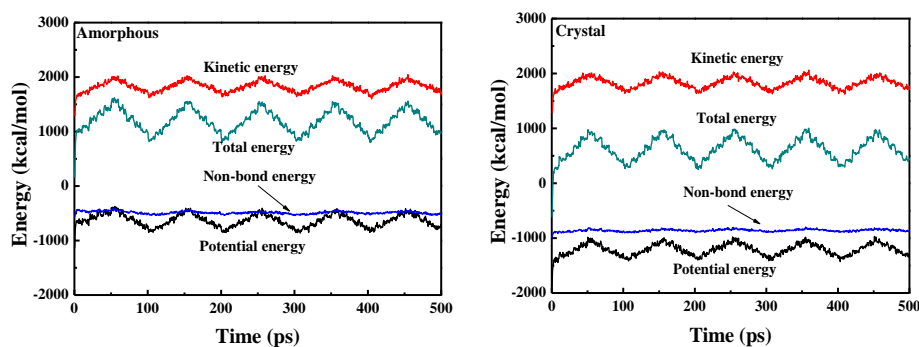


Fig. 2. Energy fluctuation of the two systems during annealing.

3. Results and discussions

3.1. Structural evolution

Solid-liquid phase transition is a process that changes from a more ordered state to a more disordered state, which means a change in molecular structure, and the free thermal movement of molecules increases. That is, the changes in the microstructure of matter can cause the change of material thermophysical properties. Therefore, it is of great significance to study the microstructure of PCMs in the process of phase transition. In this paper, the structural characteristics of *n*-octadecane molecular chain in the two systems (the system “Crystal” and the system “amorphous”) during phase transition were analyzed by the end to end distance distribution and bond torsion angle distribution.

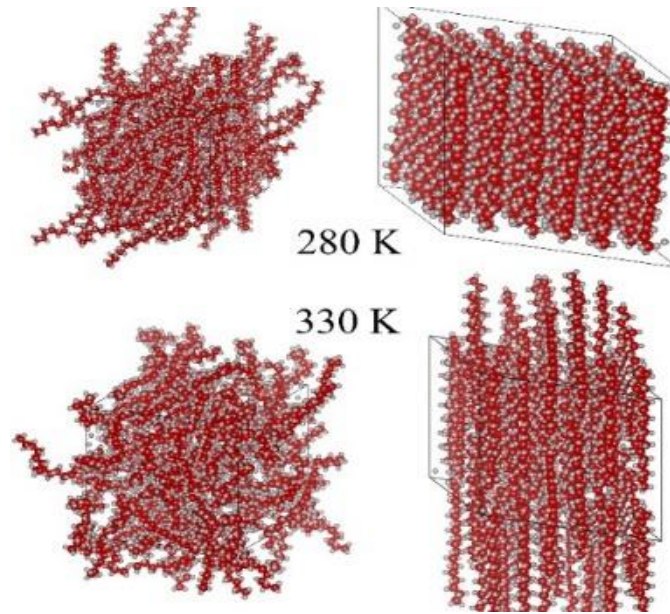


Fig. 3. The structure of two systems in solid and liquid (red balls are carbon atoms; gray balls are hydrogen atoms).

Fig. 3 shows the structure comparison of the two systems in solid state and liquid state. The end to end distance is the vector distance between the two ends of the molecular chain. The bond torsion angle is also called dihedral angle, when a single bond rotates, other bonds on the adjacent carbon will cross into a certain angle. The molecular end to end distance and C-C-C-C bond torsion angle in n-octadecane molecular chain are shown in Fig. 4.

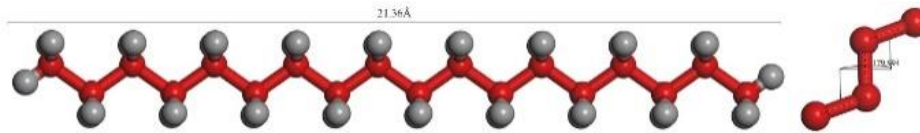


Fig. 4. End to end distance and the bond torsion angle (red balls are carbon atoms; gray balls are hydrogen atoms).

Fig. 5 and Fig. 6 show the end to end distance distribution and bond torsion angle distribution of n-octadecane system with crystalline structure and amorphous structure at different temperatures respectively. The comparison of the end to end distance distribution curve from 280 K to 330 K shows that the peak value of crystallization system curve gradually moves to the left, and the curve gradually widens and shortens, with the increase of temperature, which indicates the bending degree of chain increase and the order degree of structure decreases. When the temperature increases to 300 K ~ 310 K, the peak value of distribution curve significantly reduced, showing the system has occurred phase transition, which can also be reflected in the change of the bond torsion angle distribution curve of Fig. 5b.

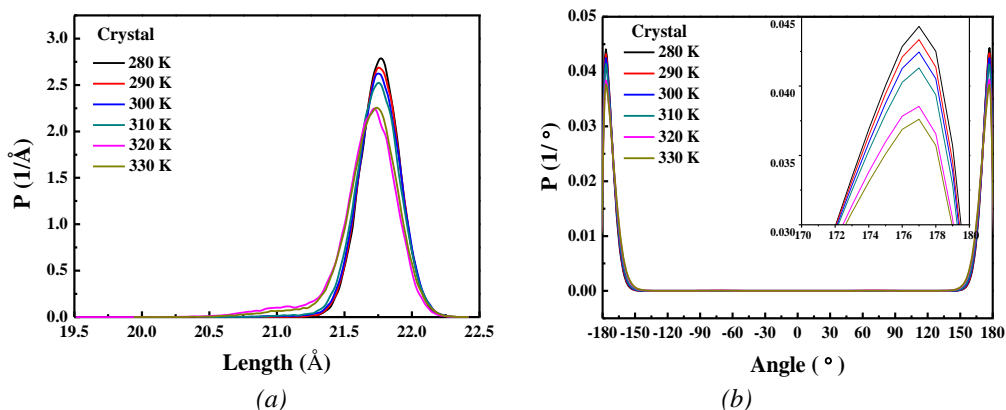


Fig. 5. End to end distribution and torsional Angle distribution of crystalline *n*-octadecane system
(a) end to end distribution; (b) bond torsion angle distribution.

For amorphous system, the end-to-end distance distribution curve can be divided into before and after phase transition two stages. Fig. 6a shows the end to end distance distribution of the system from 280 K to 300 K before the phase transition. At this temperature, the system is in a solid state without phase transition. It can be seen that the end to end distance of *n*-octadecane molecular chain mainly distributes in 17-19 Å. With the increase of temperature, the peak value of the end to end distance decreases, and the value near 12-14 Å increases. It indicates that the molecular chain configuration of the amorphous system changes from straight chain to curved state with the increase of temperature. Figure 6b shows the end to end distance distribution of the system from 310 K to 330 K after the phase transition. At this time, the system has undergone phase transition and gradually liquefied. Different from the system in solid state, the peak value of the end-to-end distance distribution of the liquid state molecular chain increases with the increase of temperature, and the peak value of end-to-end distance distribution in liquid phase is higher than that in solid state. This indicates that the end to end distance distribution of the molecular chain in the range of 17 ~ 19 Å is increased, and the *n*-octadecane molecular chain has the tendency of gradually stretching from the bending state. This phenomenon is related to the change of the specific volume of the system during the phase transition, as shown in Fig. 6d. After the phase transition, the density decreases and the specific volume increases in the liquid state. The specific volume of *n*-octadecane increases gradually because the molecular chain of *n*-octadecane is gradually stretched from the bending state with the increase of temperature.

Comparing the bond torsion angle distribution of the two systems, it can be seen that there are two different conformations in the bond torsion angle of amorphous systems: the stretching conformation near $\pm 180^\circ$ and the twisted conformation near $\pm 70^\circ$ respectively. While the bond torsion angle distribution of crystalline systems is mostly dominated by the stretching conformation, and the twisting conformation near $\pm 70^\circ$ is only slightly protrusion. Both system showed that with the increase of temperature, the peak value at $\pm 180^\circ$ decreased gradually, and the peak value at $\pm 70^\circ$ increased gradually. This phenomenon fully shows the tendency of the *n*-octadecane molecular chain of both systems gradually change to a twisted conformation with the temperature rises during the phase transition, which reflecting the change in the microstructure of both systems.

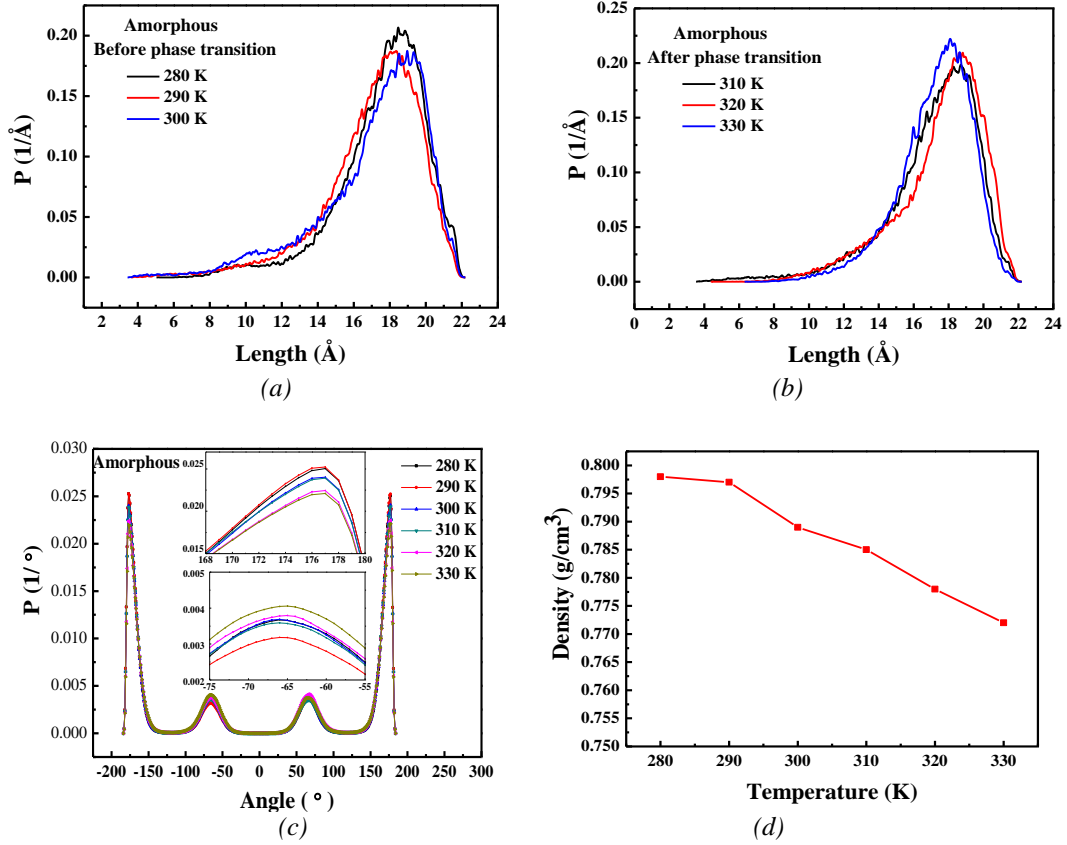


Fig. 6. Distribution of end to end distance and bond torsion angle of amorphous *n*-octadecane system: (a) Distribution of end to end distance before phase transition; (b) Distribution of end to end distance after phase transition; (c) Distribution of bond torsion angle; (d) Density changes with temperature during phase transition.

3.2. Diffusion Coefficient

For alkane-based PCMs, it is an important method by analyzing the melting point and thermal mass transport of the system to study the thermal energy storage of the PCMs. [20] The self-diffusion coefficient is an important thermophysical parameter that describes the mass transfer phenomenon in the system, [21-24] and it is usually difficult to obtain through experimental methods. In the MD simulations, usually calculated mean-square displacement (MSD) to obtain the self-diffusion coefficient of the system. The mean square displacement represents the statistical average of the particle trajectory changing with the simulation time, and is used to describe the diffusion behavior of the particles in the system, which can be expressed as:

$$MSD = \left\langle \left| \vec{r}_i(t) - \vec{r}_i(0) \right|^2 \right\rangle \quad (2)$$

According to the Einstein equation, the self-diffusion coefficient can be expressed as:

$$D = \frac{1}{6N} \lim_{t \rightarrow \infty} \frac{d}{dt} \sum_{i=1}^N \left\langle \left| r(t)_i - r_i(0) \right|^2 \right\rangle = \lim \left(\frac{MSD}{6t} \right) \quad (3)$$

where the D represents the self-diffusion coefficient; N is the number of atoms in the system; t is the simulation time; r_i represents the position vector of the i_{th} particle; and " $\langle \rangle$ " represents the statistical average of the system.

Fig. 7 shows the mean square displacement of n-octadecane at different temperatures in the two systems. It can be seen from Fig. 7a that when the temperature is lower than 300 K, the mean square displacement of the crystalline system is parallel to the X-axis, and the value is slightly greater than 0, which indicates that the molecular thermal motion in the system is very weak, the intermolecular forces play a dominant role, and the system is in solid state. When the temperature increases from 300 K to 310 K, the mean square displacement curve shows a slow upward trend with the simulation time, which indicates that the crystalline system has undergone phase transition and started to melt. When the temperature is higher than 310 K, the mean square displacement curve increases significantly with the simulation time, indicating that the crystallization system has melted into liquid state. Thus, the phase transition temperature of n-octadecane crystalline system is about 300K~310K. Fig. 7(b) shows the MSD curves of amorphous systems, unlike crystalline systems, the mean square displacement curves of amorphous systems show a trend of increasing with simulation time, and the mean square displacement values are much larger than that of crystalline systems. When the simulated temperature is higher than 310 K, the slope of the curve increases obviously, which indicates that the amorphous system has undergone phase transition, and the system melts into liquid state at this time.

Based on the mean square displacement curve of amorphous system and Einstein equation, we can get the self-diffusion coefficient of the system as shown in Fig. 8. When the material is in a single phase, the self-diffusion coefficient is a single value function of temperature, so it can be used to characterize the diffusion performance of the system at different temperatures, thus deducing the phase transition temperature of the system. When the curve of self-diffusion coefficient changes with temperature mutates, we can infer that the system undergoes phase transition. It can be seen from Fig. 8 that the self-diffusion coefficient of the amorphous system changes suddenly at 310 K, that is, the phase transition temperature of the amorphous system is about 310 K.

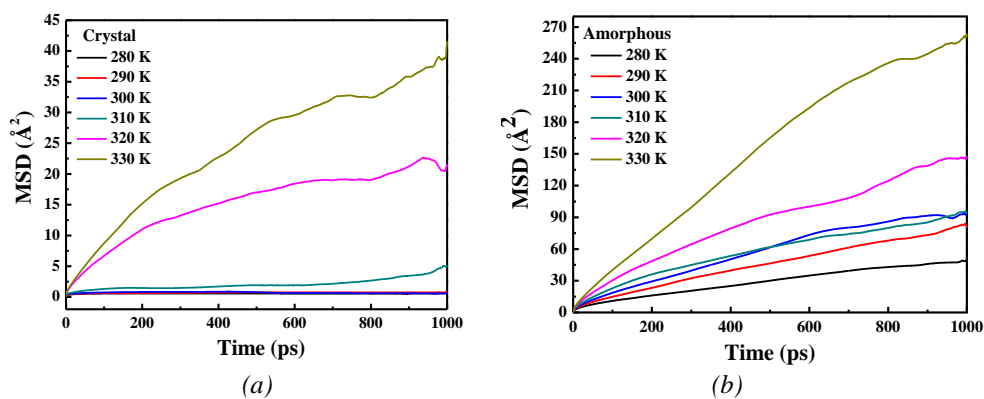


Fig. 7. Mean square displacement curve of the two systems: (a) crystalline system (b) amorphous system.

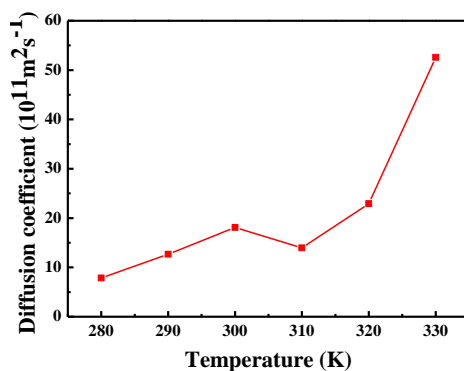


Fig. 8. Self-diffusion coefficient of n-octadecane amorphous system at different temperatures.

3.3. Thermal conductivity

Thermal conductivity is an important thermophysical parameter to measure the thermal transport performance of materials. There is no doubt that the thermal conductivity of PCMs is a bottleneck limiting the promotion and application in the field of thermal energy storage. [25] In this paper, reverse non-equilibrium molecular dynamics (RNEMD) [26,27] is used to calculate the thermal conductivity of the two systems at different temperatures based on Fourier's law of thermal conductivity:

$$K = - \frac{J_z}{\left(\frac{\partial T}{\partial z} \right)_{\text{ave}}} \quad (4)$$

J_z represents the heat flux in the Z direction, and $\partial T/\partial Z$ represents the temperature gradient along the Z axis.

The simulation box is initially divided into 20 layers along the Z axis, among which the first and last layers are heat sources, and the middle layer(N/2+1) is heat sink. Schematic diagram of the evaluation of thermal conductivity can be seen in Fig. 9.

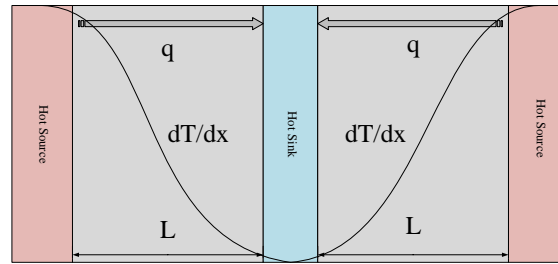


Fig. 9. Schematic diagram of the evaluation of thermal conductivity.

The thermal conductivity of n-octadecane crystalline system and amorphous system at different temperatures is shown in the Figure 10. It can be seen that the thermal conductivity of both systems in the solid state is higher than that in the liquid state, and there is a large decrease in the phase transition. Because the phase transition process destroys the relatively ordered structure in the system, which makes the liquid thermal conductivity relatively low. The PCM near the melting point is in the state of solid-liquid mixing. At the solid-liquid interface, the heat transfer efficiency of the system is reduced due to the hindered molecular thermal movement, which leads to the decrease of the thermal conductivity of the system. Comparing with Fig. 10(a) (b), the thermal conductivity of n-octadecane crystalline system is much higher than that of amorphous system, and its value is about ten times of that of amorphous system. It can be seen that improving the orderliness of the microstructure of PCMs is of great significance for improving the thermophysical properties of materials.

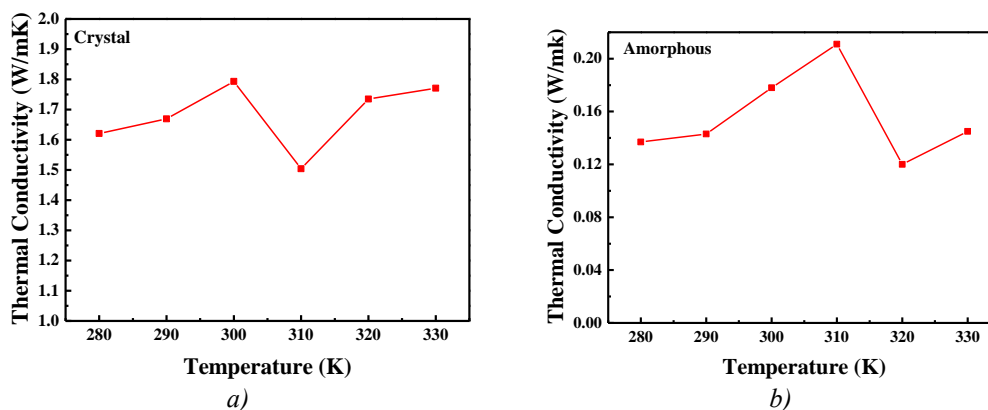


Fig. 10. The thermal conductivity of the two systems varies with temperature:
(a) crystalline system, (b) amorphous system.

4. Conclusion

From the microscopic point of view, the molecular models of crystalline n-octadecane system and amorphous n-octadecane system were established, and the microstructures and thermophysical properties of both systems during the phase transition were studied by MD simulation. The main conclusions are collected:

By comparing the amorphous system with the crystalline system, it is observed that the crystalline system has been dominated by the stretched conformation, while the conformation of n-octadecane molecular chain in amorphous system is quite different before and after the phase transition. The conformation of n-octadecane molecular chain in crystalline system is mainly stretching conformation, while the conformation of n-octadecane molecular chain in amorphous system is quite different before and after the phase transition. The molecular chain tends to bend with the increase of temperature before the phase transition, and extends gradually after the phase transition, which is also the reason for the increase of specific volume of the system.

The mean square displacement of the crystalline system is much smaller than that of the amorphous system, and is slightly greater than 0 before the phase transition. The phase transition temperature range of both systems is 300 K~310 K.

The thermal conductivity of the crystalline system is much higher than that of the amorphous system, and its value is about 10 times that of the amorphous system. Because of the phase transition process destroys the relatively ordered structure in the system, the thermal conductivity of both systems in the solid state is higher than that in the liquid state. The phase transition material near the melting point is in the state of solid-liquid mixing. At the solid-liquid interface, the heat transfer efficiency of the system is reduced due to the hindered molecular thermal movement, which leads to the decrease of the thermal conductivity of the system.

References

- [1] C. Y. Zhao, G. H. Zhang, *Renewable and Sustainable Energy Reviews* **15**(8), 3813 (2011).
- [2] M. R. Anisur, M. H. Mahfuz, M. A. Kibria, R. Saidur, I. H. S. C. Metselaar, T. M. I. Mahlia, *Renewable and Sustainable Energy Reviews* **18**(Feb), 23 (2013).
- [3] C. Z. Liu, Z. H. Rao, Y. M. Li, *Energy Technology* **4**, 496 (2016)
- [4] K. S. Reddy, V. Mudgal, T. K. Mallick, *Journal of Energy Storage* **15**(Feb), 205 (2018).
- [5] Z. A. Qureshi, H. M. Ali, S. Khushnood, *International Journal of Heat and Mass Transfer* **127**(PT.C), 838 (2018).
- [6] Z. H. Rao, S. F. Wang, F. F. Peng. *International Journal of Heat and Mass Transfer* **64**(sep),

- 581 (2013).
- [7] W. L. Cheng, W. W. Li, Y. L. Nian, W. D. Xia, *International Journal of Heat and Mass Transfer* **116**, 507 (2018).
- [8] J. N. Shi, M. D. Ger, Y. M. Liu, Y. C. Fan, N. T. Wen, C. K. Lin, N. W. Pu, *Carbon* **51**, 365 (2013).
- [9] Y. Wang, R. Yang, Y. Cheng, Y. Y. Zhang, *RSC Advances* **5**(101), 82638 (2015).
- [10] C. D. Nie, X. Tong, S. Y. Wu, S. G. Gong, D. Peng, *Rsc Advances* **5**(113), 92812 (2015).
- [11] N. Sahan, M. Fois, H. Paksoy, *Solar Energy Materials and Solar Cells* **137**, 61 (2015).
- [12] T. Jiang, X. Zhang, S. Vishwanath, X. Mu, V. Kanzyuba, D. A. Sokolov, S. Ptasinska, D. B. Go, H. Xing, T. Luo, *Nanoscale* **8**(21), 10993 (2016).
- [13] A. Karaipekli, A. Bicer, A. Sari, V. V. Tyagi, *Energy Conversion and Management* **134**, 373 (2017).
- [14] S. Y. Yu, X. D. Wang, D. Z. Wu, *Applied Energy* **114**(2), 632 (2014).
- [15] Y. R. Huang, P. H. Chuang, C. L. Chen, *Transfer* **91**(dec.), 45 (2015).
- [16] H. Babaei, P. Keblinski, J. M. Khodadadi, *International Journal of Heat and Mass* **58**(1-2), 209 (2013).
- [17] X. J. Liu, C. P. Lin, Z. H. Rao, *Journal of the Energy Institute* **90**(4), 534 (2017).
- [18] H. Sun, *Journal of Physical Chemistry B* **102**, 7338 (1998).
- [19] X. J. Liu, Z. H. Rao, *Journal of the Energy Institute* **92**(1), 1 (2017)
- [20] Q. B. Li, Y. S. Yu, Y. L. Liu, C. Liu, L. Y. Lin, *Materials (Basel)* **10**(1), 38 (2017).
- [21] Z. H. Rao, S. F. Wang, F. F. Peng, *International Journal of Heat and Mass Transfer* **66**, 575 (2013).
- [22] M. X. Zhang, C. L. Wang, A. L. Luo, Z. H. Liu, X. S. Zhang, *Applied Thermal Engineering* **166**, 114639 (2019).
- [23] P. Yuan, P. Zhang, T. Liang, S. P. Zhai, *Applied Surface Science* **485**, 402 (2019).
- [24] P. Yuan, P. Zhang, T. Liang, S. P. Zhai, D. G. Yang, *Journal of Materials Science* **54**(2), 1488 (2019).
- [25] X. Tong, S. Y. Wu, D. Q. Peng, S. G. Gong, *Phase Transitions* **89**(6), 598 (2016).
- [26] E. Lussetti, T. Terao, F. Müller-Plathe, *Journal of Physical Chemistry B* **111**(39), 11516 (2007).
- [27] Florian Müller-Plathe, *Journal of Chemical Physics* **106**(14), 1997.